The excellent specifications of the isolated squirrel cage self-excited induction generator (SEIG) make it the first choice for use with renewable energy sources. However, poor voltage and frequency regulation (under load and speed perturbations) are the main problems with isolated SEIGs. Wide dependence on the SEIG requires prior knowledge of its behaviour with regard to variations in the input of mechanical power and output of electrical power to develop a control system that is capable of maintaining the voltage and frequency at rated values, as far as possible, with any change in the input or output power of the SEIG. In this paper, a mathematical model of a wind energy conversion system (WECS) based on a squirrel cage SEIG with a generalized impedance control (GIC) was built using the Matlab/Simulink environment in a d-q stationary reference frame. A fuzzy logic controller (FLC) was used to control the parameters of the GIC. The training of the FLC was conducted by a neural network through Matlab's Neuro-Fuzzy designer. The results of this paper showed that the trained FLC succeeded in controlling the real and reactive power flow between the SEIG and the GIC system, in which the maximum variation for both magnitude and frequency of the generated voltage with any load or wind speed perturbation will not exceed (0.2 %) for the frequency and (3 %) for the voltage magnitude in both directions. The SEIG model was validated by comparing the results obtained with those of well-known studies with the same rating and operating conditions

Keywords: induction generator, wind turbine, isolated system, dynamic model, ANFIS, GIC

UDC 621.313.332
DOI: 10.15587/1729-4061.2020.213246

MODELLING AND SIMULATION OF SELF-EXCITED INDUCTION GENERATOR DRIVEN BY A WIND TURBINE

Ammar Shamil Ghanim
Senior Engineer
E-mail: ammarshamilhanon@uomosul.edu.iq
Ahmed Nasser B. Alsammak
Doctor of Engineering Sciences, Assistant Professor, Head of Department*
E-mail: ahmed_alsammak@uomosul.edu.iq
*Department of Electrical Engineering
College of Engineering
University of Mosul
Al-Majmoaa str., Mosul, Iraq

Received date 05.10.2020
Accepted date 17.11.2020
Published date 21.12.2020

1. Introduction

The reduction of greenhouse gas emissions is crucial because of the rising need for clean and unconventional energy, especially when the depletion of fossil fuel supplies in the world is considered. As one of the exceptionally famous assets of unconventional energy, wind energy is currently seeing rapid improvements worldwide [1]. This type of power generation needs machines with variable speeds, such as asynchronous machines. Investigations have shown that almost 48.62 % of the WT generators being utilized in the industry are double-fed induction generators (DFIG), while 48.1 % are squirrel cage induction generators (SCIGs) [2]. Artificial intelligence technology offers a wide range of choices for the enhancement of complex control systems. In addition to control systems, the adaptive neuro-fuzzy algorithm may be used for the modelling of complex systems, as in the paper [3].

The scientific relevance of this work is the study and analysis of a wind energy conversion system based on an induction generator that is controlled by a GIC-FLC.

The importance of the modelling comes from the ability to obtain a wide range of analyses for the transient and steady-state responses in different operating conditions without side effects like overheating or excessive mechanical strength, which may accompany the actual testing, etc. The developed SEIG wind turbine model can be the basis for the design of various control schemes and the estimation of their combined performance [4].

2. Literature review and problem statement

Self-excited squirrel cage induction machines have been the preferred choice for use with wind turbines in remote areas due to their rugged construction, low maintenance, and low cost in addition to their capacity to withstand short-circuiting and overloading [5, 6].

Although induction generators can generate active power, they are unable to produce the reactive power needed for their excitation in addition to supplying an inductive load. Therefore, an excitation source must be available as a capacitor bank, and this is generally determined to ensure that the terminal voltages are evaluated under no-load conditions and at a known frequency [7, 8].

A d-q model of a SEIG and its simulation by means of a simulation software known as 'SIMNON' were presented by [9]. The wind turbine used was presented with its output torque characteristics at a fixed wind speed that was approximated using a fifth-order polynomial curve. The response of this system to variations in the wind speed could not be checked with this representation of a wind turbine, and no control system was employed in this study.

Transient analysis of a SEIG model connected to a wind turbine with fixed, step, and random variations of wind speed was implemented by [10]. This system works in an open-loop state.

The main problem with the use of the SEIG in wind turbines is the poor voltage regulation as well as variations

in the frequency, both of which result from changes in consumer consumption and wind speed [11, 12].

The system proposed by [13] consisted of a photovoltaic cell, battery, and a STATCOM. Both a PI and FLC were employed to control the STATCOM. The model was able to control both the voltage and frequency with variations in the load or wind speed.

A PWM voltage source converter connected to a battery on a DC bus side was used by [14] to control both the frequency and voltage of an induction generator. This was done by controlling the flow of active and reactive power between the converter and generator. The converter was controlled by means of a proportional-integral (PI) controller.

Both [13, 14] made use of the SimPowerSystems (SPS) toolbox and not a mathematical model. In the case where a mathematical model is used with a PI controller, a linearization process must be done to effectively tune the parameters of the PI controller [15].

To control the voltage and frequency of the SEIG, [16] presented a mathematical model of the STATCOM-battery storage, while [17] called the latter arrangement a generalized impedance control (GIC), and presented it using a power system block set with Matlab/Simulink. Both studies made no mention of the control strategy of the GIC, which means that it works with open-loop control.

In addition to the use of a PI controller with the GIC, [18] also used a voltage sensor to measure the voltage. The magnitude of the peak voltage was calculated using the Coordinate Rotation Digital Computer (CORDIC) algorithm. This peak voltage was passed to a comparator and finally, to the PI controller. In this paper, no mention was made to the turbine model, also it depended on the PI controller, which would then have required a linearization process to tune the parameters of the PI controller, as mentioned in [15].

It was clear from the abovementioned works that a more detailed study was required with regard to a complete mathematical model of a controlled wind energy conversion system that can be considered as the basis for any dynamic study or development of control systems.

3. The aim and objectives of the study

The aim of this research is to develop a mathematical model for a SEIG driven by a WT, followed by the analysis of the dynamic response with the variation in both wind speed and SEIG electrical load, also to develop a control system capable of maintaining both voltage and frequency constants at rated values, all of that through simulations using the MATLAB/Simulink environment.

To achieve this aim, the following research objectives were set:

– representing the mathematical model of the SEIG in the d-q stationary reference frame, and simulating it with considering the prime mover as a constant speed;

– designing and representing the mathematical model of the wind turbine (WT) that was compatible with the machine rating, and simulating it as a prime mover for the SEIG;

– designing and representing the mathematical model of the GIC in the d-q stationary reference frame with employing the FLC in controlling its control parameters, and then use the FLC-GIC to control the WT-SEIG model through simulation.

4. Design, modelling, and control of the WECS

The research was carried out by representing the mathematical model of WECS with Matlab/Simulink. For this purpose, a set of equations was derived and arranged to model the system in the Matlab/Simulink environment. The ratings of both wind turbine and GIC will be designed according to the rating of the machine.

4. 1. SEIG model

A stationary d-q axes reference frame was used to model the dynamics of the three-phase squirrel cage induction generator. The d-q equivalent circuit of the machine with the excitation capacitor is shown in Fig. 1. Eight first-order differential equations, which describe the relationship between the rotor and stator of the machine, were used to model the SEIG.

Several assumptions had to be considered in the modelling of SEIG:

– iron losses in the machines were neglected;

– the magnetizing inductance was considered a function of RMS phase voltage (V_{ph}), while the other machine parameters were considered constants;

– both the time harmonics within the initiated voltage and current waveforms, also the space harmonics within the magnetomotive force, were ignored;

– the rotor, stator, and load leakage reactance corresponded with the rated frequency.

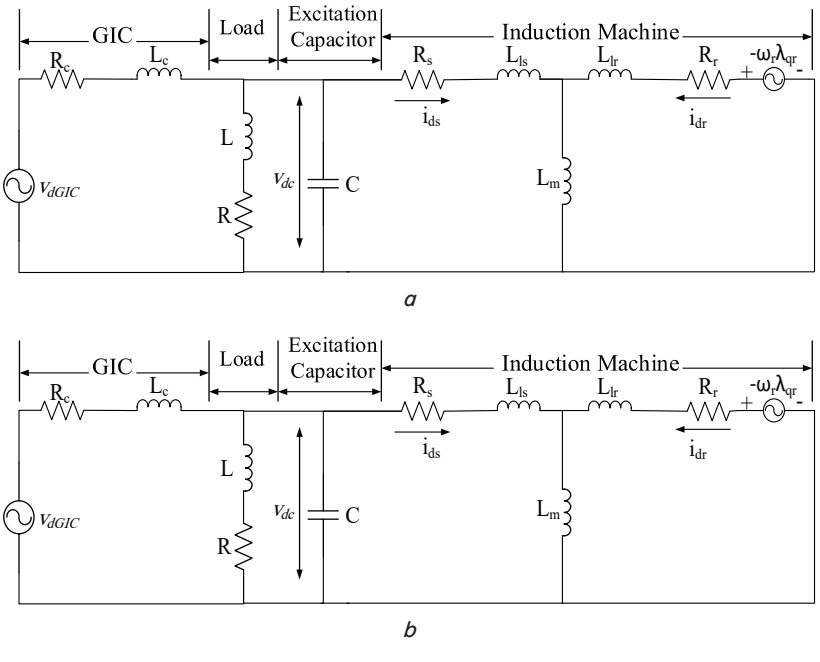

Fig. 1. d-q model of SEIG, load, and GIC: *a* – q-axis, *b* – d-axis

The following differential equations were derived from Fig. 1 (while excluding the GIC section for now), and these were then used with Matlab/Simulink to obtain the SEIG model [19]:

$$\frac{di_{qs}}{dt}=\left(\frac{1}{L_m{}^2-L_sL_r}\right)\begin{pmatrix}L_rR_si_{qs}+L_m{}^2\omega_ri_{ds}-L_mR_ri_{qr}+\\+L_m\omega_rL_ri_{dr}+L_rv_{qc}+L_mK_q\end{pmatrix}; \quad (1)$$

$$\frac{di_{ds}}{dt}=\left(\frac{1}{L_m{}^2-L_sL_r}\right)\begin{pmatrix}-L_m{}^2\omega_ri_{qs}+L_rR_si_{ds}-L_m\omega_rL_ri_{qr}-\\-L_mR_ri_{dr}+L_rv_{dc}-L_mK_d\end{pmatrix}; \quad (2)$$

$$\frac{di_{qr}}{dt}=\left(\frac{1}{L_m{}^2-L_sL_r}\right)\begin{pmatrix}-L_mR_si_{qs}-L_m\omega_rL_si_{ds}+L_sR_ri_{qr}-\\-L_s\omega_rL_ri_{dr}-L_mv_{qc}-L_sK_q\end{pmatrix}; \quad (3)$$

$$\frac{di_{dr}}{dt}=\left(\frac{1}{L_m{}^2-L_sL_r}\right)\begin{pmatrix}L_mL_s\omega_ri_{qs}-L_mR_si_{ds}+L_s\omega_rL_ri_{qr}+\\+L_sR_ri_{dr}-L_mv_{dc}+L_sK_d\end{pmatrix}; \quad (4)$$

$$\frac{dv_{qc}}{dt}=\frac{i_{qs}-i_{ql}}{C}; \quad (5)$$

$$\frac{dv_{dc}}{dt}=\frac{i_{ds}-i_{dl}}{C}; \quad (6)$$

$$\frac{di_{ql}}{dt}=\frac{v_{ql}-Ri_{ql}}{L}; \quad (7)$$

$$\frac{di_{dl}}{dt}=\frac{v_{dl}-Ri_{dl}}{L}, \quad (8)$$

where v and i are the instantaneous voltage and current, respectively; L_s is the stator self-inductance; L_r is the rotor self-inductance; L_m is the mutual inductance; L is the inductive load; R is the resistive load; C is the excitation capacitance; ω_r is the generator speed; k_d and k_q are constants that represent the initial induced voltage along the d-axis and q-axis, respectively due to the remnant magnetic flux in the core. The subscripts d and q were used for the direct and quadrature axes, respectively; the subscripts s and r were used for the stator and rotor variables, respectively; while the subscript l was used for the leakage components that came with L and for the load which came with v or I; and the subscript c was used for the excitation capacitance.

The magnetizing inductance played a major role in the build-up and stabilization of the voltage of the self-excited induction generator. Before the model could be run, a formula for the magnetizing inductance in terms of the magnetizing current or air gap voltage had to be provided, because the magnetizing inductance of the induction generator was nonlinear. The relationship between the magnetizing inductance and phase voltage was found by means of a synchronous impedance test. Then, with the use of the Matlab Curve Fitting Tool, a polynomial, which represents the dynamic magnetizing inductance, has been obtained. The specifications and parameters of the squirrel cage induction generator used in this study are 3 phase, Y-connected, 3.6 kW, 415 V, 7.8 A, 4-pole, 50-Hz, squirrel-cage, R_s=1.7Ω, R_r=2.7Ω, L_{ls}=L_{lr}=11.4 mH, while the dynamic magnetizing inductance is described as:

$$L_m=-1.62\times10^{-11}V_{ph}^4+2.67\times10^{-8}V_{ph}^3-\\-1.381\times10^{-5}V_{ph}^2+1.76\times10^{-3}V_{ph}+0.23, \quad (9)$$

where V_{ph} is the phase voltage [9].

4. 2. Design and modelling of wind turbine (WT)

The air mass power, P_w that flows through an area A at a speed of V_w can be calculated by:

$$P_w=0.5\rho AV_w{}^3, \quad (10)$$

where ρ is the air density in kg/m^3, and A is the blade swept area in m^2. The amount of air mass power extracted by the turbine blades and converted into mechanical power, (P_t) in watts in the shaft of the system can be calculated as:

$$P_t=0.5\rho AV_w^3C_p, \quad (11)$$

where C_p, which is dimensionless and nonlinear, represents the aerodynamic efficiency of the wind turbine and can be calculated as:

$$C_p(\lambda,\beta)=0.5176\left(\frac{116}{\lambda_i}-0.4\beta-5\right)e^{\frac{-21}{\lambda_i}}+0.0068\lambda, \quad (12)$$

where $\frac{1}{\lambda_i}=\frac{1}{\lambda+0.08\beta}-\frac{0.035}{1+\beta^3}$, β is the blade pitch angle in degrees, and λ is the tip speed ratio (the ratio between the speeds of the turbine blade tip and the wind) and can be calculated as:

$$\lambda=\frac{R\times\omega_{tr}}{V_w}, \quad (13)$$

where R is the radius of the turbine in meters, and ω_{tr} is the speed of the turbine in Rad/s [20].

The wind turbine was designed for 3.6 kW at 9 m/s, which was regarded as the rated wind speed [21].

The designed turbine had the following specifications:

– if the speed of the turbine increases beyond the maximum designed wind speed (which was 9 m/sec here), then a mechanical control system that controls the blade pitch angle must be used to avoid exceeding the designed rated power of the turbine;

– if the speed drops to 7 m/sec, then the turbine will fail to deliver the required torque to the system;

– in the absence of a load, the system will start to work with no GIC, and the turbine torque will be greater than the machine torque without a load. Therefore, the machine will accelerate at a dangerous speed. To avoid this, a blade pitch angle control system must be designed to control the speed of the turbine. In this model, a lookup table for controlling the blade pitch angle was prepared for use to maintain the speed of the turbine at the start of operations within safe limits.

The design parameters for the wind turbine are rated power of 3.6 kW, blade length of 2.382 m, rated wind speed of 9 m/sec, and gearbox ratio of 5.3, at air density of 1.1544 kg/m^3. Fig. 2 shows the turbine performance curve (at β=0).

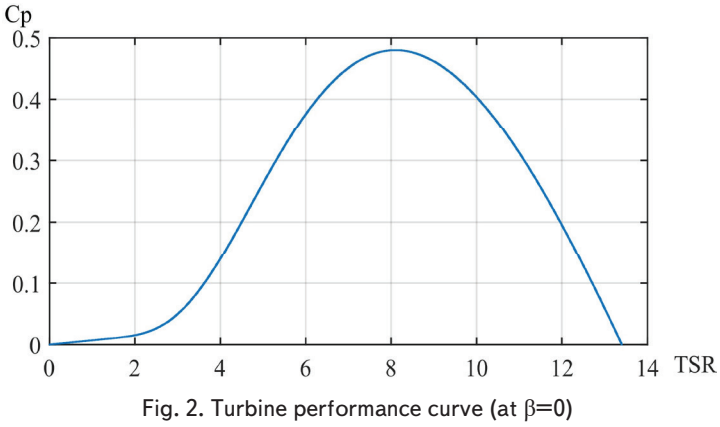

Fig. 2. Turbine performance curve (at β=0)

Note from Fig. 2 that maximum performance (C_p=0.48) occurred at β=0 and λ=8.1.

4. 3. Drive train model

The electromagnetic torque (T_e) of the induction generator can be calculated as:

$$T_e = \left(\frac{3}{2}\right) \times \left(\frac{P}{2}\right) \times L_m \left(i_{qs} \times i_{dr} - i_{ds} \times i_{qr}\right), \quad (14)$$

where P is the number of poles. The formula that connects the turbine torque with the electromagnetic torque produced by the induction generator is given by:

$$T_t = J\frac{d\omega_m}{dt} + D\omega_m + T_e, \quad (15)$$

where T_t is the turbine output torque measured at the generator shaft in N·m, ω_m is the angular mechanical rotor speed in Rad/s, D is the coefficient of friction in reference to the generator shaft in Nm/(Rad/s), and J is effective inertia in reference to the generator shaft in kg·m^2. By using (14), (15), the model of the drive train can be obtained.

4. 4. Design and modelling of generalized impedance control (GIC)

As mentioned before; the main problem with the SEIG is the poor voltage regulation in addition to the frequency variation, both of which occur as a result of changes in consumer consumption and wind speed. To solve this issue, this study employed a GIC that was controlled by an FLC.

The GIC consisted of a three-phase pulse width modulated bidirectional voltage source inverter with a battery at the dc-link side, while the ac side contained a coupling inductance, L_c to model the leakage reactance of the coupling transformer, and at the same time, to form the first-order low-pass filter, which minimized the current harmonics injected to the SEIG terminals. To model the losses of the coupling inductance, a resistance, R_c was added.

A GIC can control both the active and reactive power of a wind energy conversion system, depending on the value of the modulation index (MI) of the PWM inverter and the phase angle, δ, between the fundamental component of the inverter output voltage (V_{GIC}) and the SEIG terminal voltage (Vg).

From the equivalent circuit shown in Fig. 1, the following differential equations, which describe the GIC model in the stationary reference frame, can be derived:

$$\frac{di_{d\mathrm{GIC}}}{dt} = -\frac{R_c}{L_c} i_{d\mathrm{GIC}} - \frac{v_{d\mathrm{GIC}}}{L_c} + \frac{v_{ds}}{L_c}; \quad (16)$$

$$\frac{di_{q\mathrm{GIC}}}{dt} = -\frac{R_c}{L_c} i_{q\mathrm{GIC}} - \frac{v_{q\mathrm{GIC}}}{L_c} + \frac{v_{qs}}{L_c}, \quad (17)$$

where the subscript '$_{\mathrm{GIC}}$' refers to the controller variable. The GIC output voltages can be calculated by:

$$v_{q\mathrm{GIC}} = MI \times K \times V_B \times \sin(\omega t + \delta); \quad (18)$$

$$v_{d\mathrm{GIC}} = MI \times K \times V_B \times \cos(\omega t + \delta), \quad (19)$$

where K is the coupling transformer turns ratio, V_B is the battery voltage, MI is the modulation index and ωt is the generator voltage angle. The overall equivalent circuit of the induction generator, excitation capacitor, load, and GIC in the d-q stationary reference frame is shown in Fig. 1 [16]. The parameters of the GIC, which was designed according to machine ratings and the maximum boundary of operation [22], are L_c=100 mH, R_c=1.64Ω, V_B=700 volts, and K=0.857.

4. 5. Control of GIC by fuzzy logic controller (FLC)

The GIC was controlled using two FLCs; one for controlling the MI, and the other for controlling δ. Generating and training of the related fuzzy inference systems (FIS)s were done through Matlab's Neuro-Fuzzy Designer. Table 1 shows the training information for both controllers.

Fig. 3 shows screenshots of the training process with Matlab's Neuro-Fuzzy Designer.

The inputs-outputs data used for the training process had been obtained through excessive simulations of the SEIG-WT-GIC model.

Table 1

Information on the training of (FIS)s

ANFIS information for control angle (δ) FIS	
Number of inputs	4
Number of membership functions (*Mf*)s for each input	5
Type of (*Mf*)s	gaussian
Number of training epochs	7
Error at the end of the training	0.0109
Number of training data pairs	5,946
ANFIS information for (*MI*) FIS	
Number of inputs	3
Number of membership functions (*Mf*)s for each input	9
Type of (*Mf*)s	gaussian
Number of training epochs	7
Error at the end of the training	0.0017
Number of training data pairs	5,946

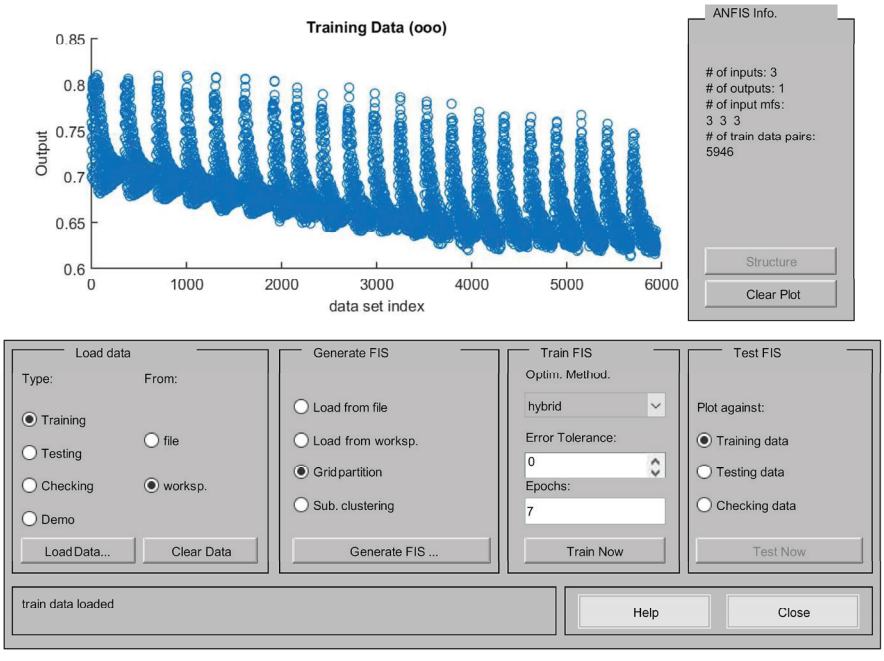

a

b

Fig. 3. Screenshots of the training process with Matlab's Neuro-Fuzzy Designer for: *a* — modulation index FIS; *b* — delta angle FIS

5. Results of different simulations

5. 1. Response of the SEIG model driven by a constant speed

Fig. 4 shows the generated $v(t)$ of the proposed model without a load and with an excitation capacitance equal to 60 μF, at a constant rotor speed of 1465 rpm.

Fig. 5, 6 show the voltage and output power respectively of the proposed model with a load of 55 Ω, with the same excitation capacitance, at a constant speed of 1480 rpm.

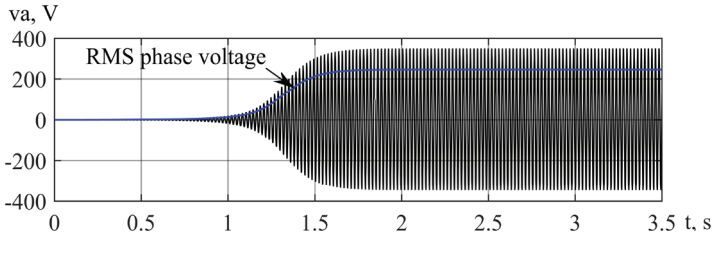

Fig. 4. Instantaneous and RMS phase voltage of the proposed model

It is worth mentioning that these waveforms covered the dynamics for both the voltage build-up and loading.

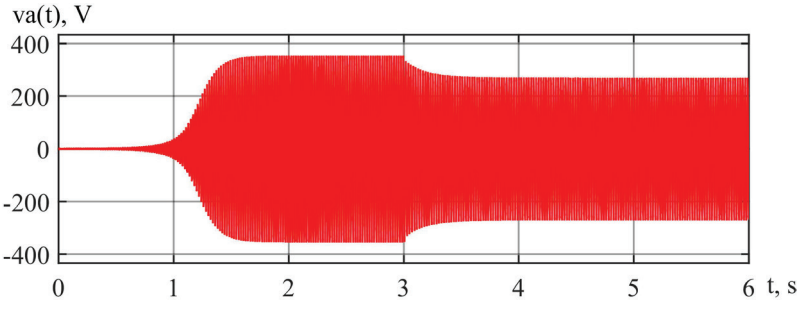

Fig. 5. Instantaneous generated voltage

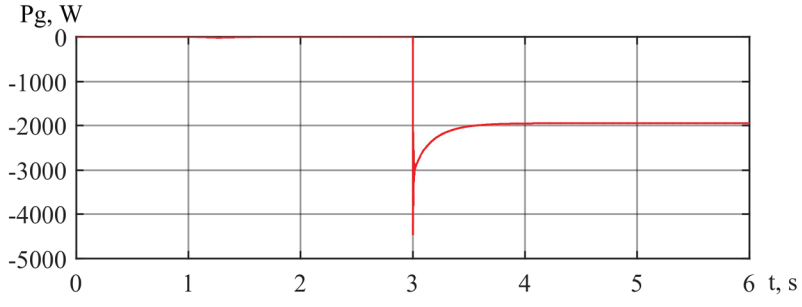

Fig. 6. Generator output power

5. 2. Response of the SEIG model driven by the wind turbine (WT) model

Fig. 7 shows the response of the designed wind turbine for different wind speeds, while Fig. 8 shows the output voltage of the SEIG model when driven by this turbine and for the same change of wind speed, at no load.

Fig. 9 shows the different waveforms for the WT-SEIG model at load and speed perturbations. According to the dynamics, the analysis will be as follows.

With the start of the simulation, the voltage started to build up with no load, and the turbine power was reduced by the pitch angle control (through the use of a lookup table) to the value required by the generator to run without a load at a frequency that was close to rated frequency.

At t=4 sec, a load of 100Ω was inserted, at the same time the value of pitch angle (β) became zero, which means that the turbine power is fully utilized. There was a drop in the voltage value because the load current reduces the share of capacitance current in the stator current according to (5), (6).

At t=6 sec, the wind speed was raised from 7 to 7.3 m/s. Both frequency and voltage increased. The increase in voltage occurred because the required capacitance value for producing the rated voltage was reduced by the increase in wind speed for the same load value, therefore, with the value of capacitance remaining unchanged here, the voltage was raised [23].

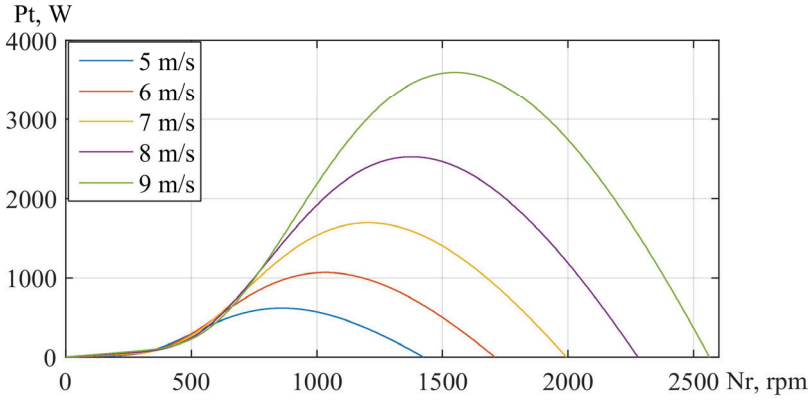

Fig. 7. Wind turbine characteristics for different wind speeds

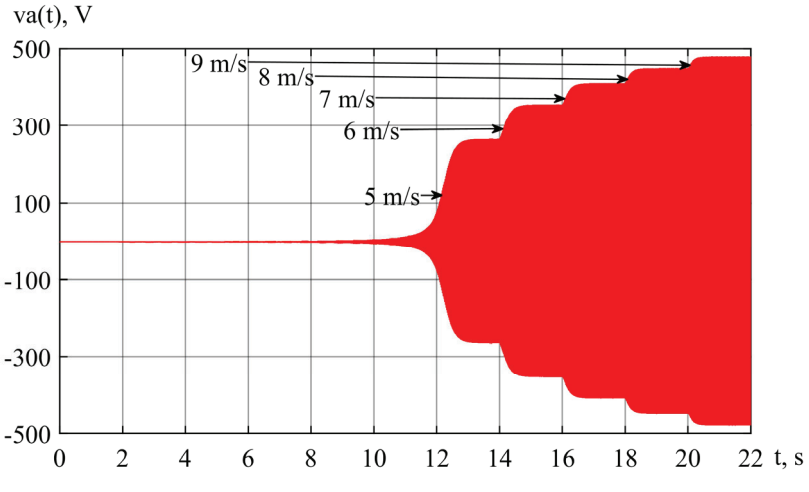

Fig. 8. SEIG output voltage for a step-change in wind speed

At t=8 sec, the resistance value decreased to 70 Ω; both voltage and frequency decreased. The decrease in voltage also occurred according to (5), (6), while the decrease in the frequency occurred as a result of the decrease in rotor speed according to (15), in which that the electromagnetic torque is increase with the turbine torque is the same.

For other periods, the same analyses can be done.

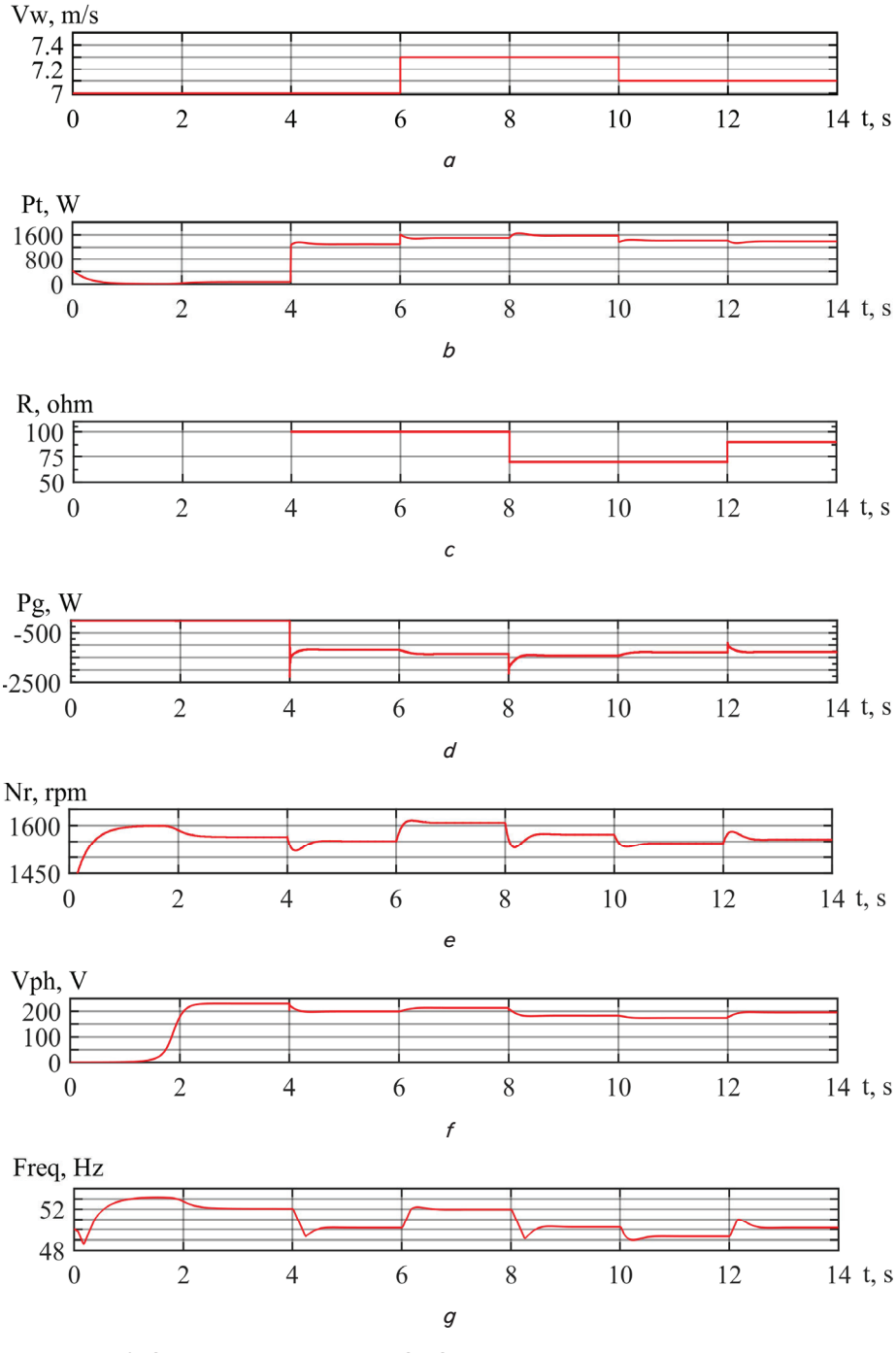

Fig. 9. Simulation results of WT-SEIG: *a* — wind speed, *b* — turbine power, *c* — load resistance, *d* — generated power, *e* — rotor speed, *f* — RMS phase voltage, *g* — voltage frequency

5. 3. Response of the WT-SEIG model controlled by GIC-FLC model

With a step-change in both wind speed and resistive –inductive load; the results of the simulation of the controlled WECS are shown in Fig. 10, 11 below, and the analysis will be as follows: with the start of the simulation; the voltage started to build up with no load, no GIC, while the turbine power was reduced by the pitch angle control (through the use of a lookup table) to the value that was required by the generator to run with no load at a frequency that was close to the rated frequency when the value of wind speed equal to 9 m/s.

At t=3 sec, with wind speed equal to 9 m/s; both the GIC and the load of 55 Ω, 10 mh are inserted into the system, also at the same time, the value of pitch angle (β) will be zero which means that the turbine power is fully utilized. The voltage rises to the rated value because the GIC delivered the required reactive power to the generator and inductive load. The frequency is equal to the rated value, with a small real power absorbed by the GIC, because of the almost balance between the input-output power of the system.

At t=6 sec, with the same values for resistive load and wind speed, the value of inductive load increased to 37 mh, and in order to maintain the rated value of voltage, the value of MI increased by the FLC to increase the reactive power supplied by the GIC. The increased impedance, in turn, decreased the real power absorbed by the load, and then to maintain the frequency at the rated limit; the FLC of delta made it with a more negative value so that the GIC absorbs an active power from the generator.

At t=8 sec, another increase in the inductive load happens, and the analysis is the same as the previous change.

At t=10 sec, with the same value of both inductive and resistive load, the wind speed decreased to 8.63 m/s. As the turbine power decreased, the generator power also decreased, and this, in turn, decreased the reactive power demand of the generator. The additional reactive power supplied by the GIC decreased from the last change, with the decrease of MI value, while the active power absorbed by the GIC became almost zero, which means no surplus active power at this values of wind speed and load, so that the value of control angle is almost zero.

At t=12 sec, another decrease in the wind speed happens, and the analysis is the same as the previous change.

From t=14 sec, until the end of the simulation, the change happens only with the resistance load, so the analysis will be with the last period only.

At t=18 sec, the value of resistive load increased from 74 Ω to 85.5 Ω, with no change for inductive load or wind speed. The active power of the load was decreased for the same active power of the turbine and generator. To prevent the rise in the frequency, the delta angle of the FLC became more negative, which meant that the GIC absorbed more real power in charging the battery. Although the value of the inductive load was kept constant in this case, the reactive power that was delivered to it decreased with the decrease in the active load power, so that the MI, in this case, was decreased to decrease the reactive power supplied by the GIC.

All the results above had been obtained by employing the fourth-order (Rung-Kutta) as a numerical integration method with an appropriate step size.

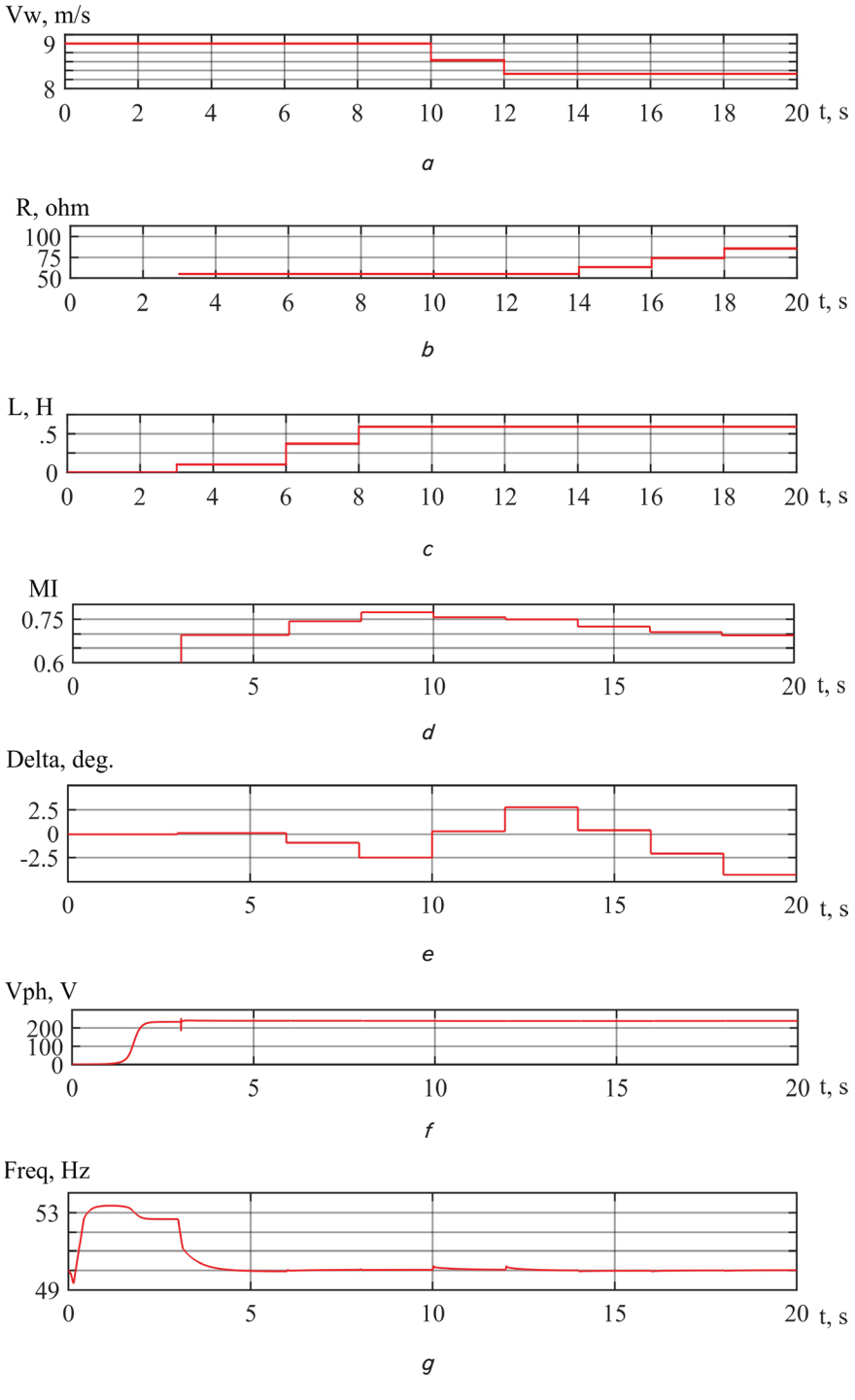

Fig. 10. Simulation results of WT-SEIG controlled by GIC-FLC: *a* — wind speed, *b* — load resistance, *c* — load inductance, *d* — modulation Index, *e* — control angle (δ), *f* — RMS of generated voltage, *g* — frequency of the generated voltage

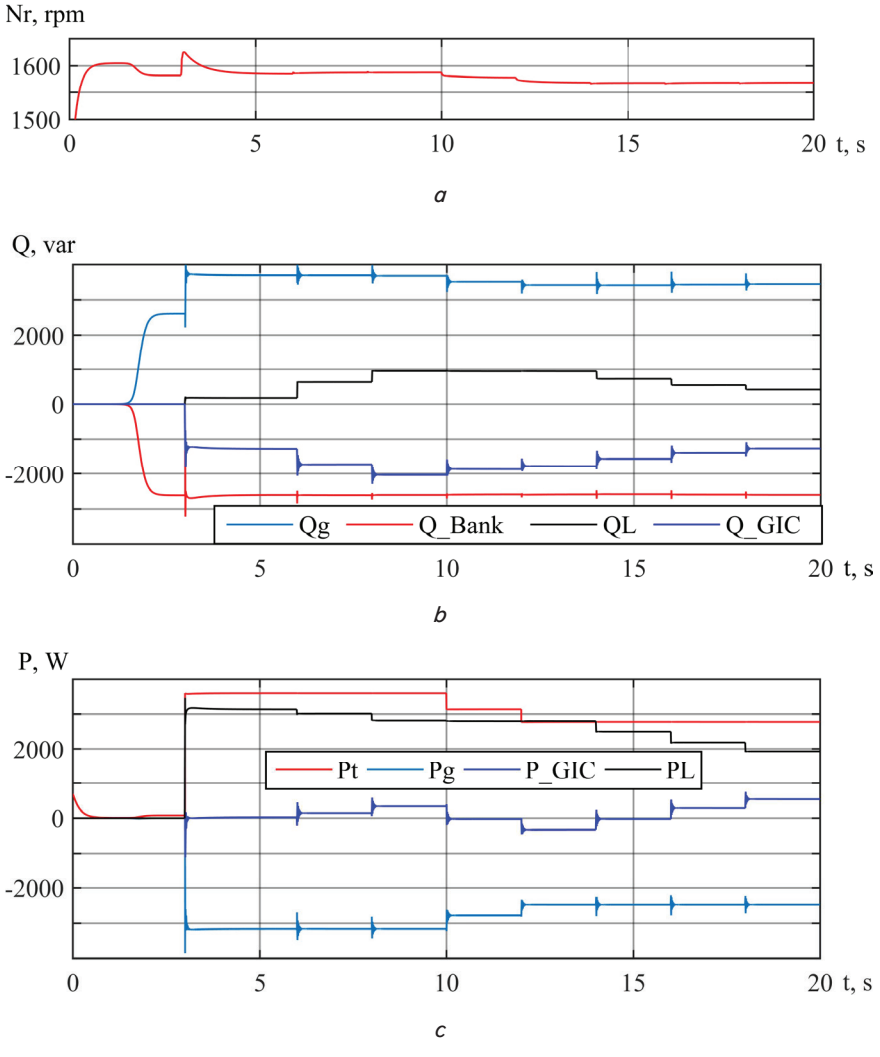

Fig. 11. Simulation results of WT-SEIG controlled by GIC-FLC: *a* — rotor speed, *b* — reactive power ('g' for generator, 'Bank' for capacitive excitation bank, 'L' for load), *c* — active power ('t 'for turbine)

6. Discussion of results

Explanations of the results are as follows:

– results with subsection (5. 1) had explained the dynamics for both voltage build-up and load insertion;

– results with subsection (5. 2) had explained the influence of both load and wind speed perturbation on the magnitude and frequency of generated voltage, also the results show the influence of load change on the rotor speed;

– results with subsection (5. 3) had explained the effectiveness of the GIC-FLC in maintaining the magnitude and frequency of generated voltage with rated values despite load and wind speed perturbations.

For the validation of the SEIG model, a comparison was made between a model from a well-known study [9], and the results shown in subsection (5.1), at the same rating and operating condition.

The proposed mathematical model succeeded in:

– gathering the required information for recognizing the behavior of the SEIG under load and wind speed perturbation as shown in Fig. 9;

– design a control system capable of maintaining both magnitude and frequency of the generated voltage as shown in subsection (5.3), which happened due to training of (FIS)s by the wide input-output data set gained from excessive simulations of the SEIG-WT-GIC.

The main advantages of the study are:

– the machine parameters were isolated from the excitation capacitor and load parameters that assisted in the study and analysis of different responses;

– the complete mathematical model for the WECS, including the controllers, gives the ability to know more about each variable in the input and its influence on each variable in the output;

– the dynamic change of each variable of the SEIG like magnetizing inductance, flux, rotor current can be easily measured, which are difficult to measure them in practice;

– with the employing of the FLC in control of the parameters of the GIC, there is no need for linearization of the mathematical model, in comparison with the conventional PID controller, which required that linearization for the tuning of PID parameters.

When constructing the mathematical model of the SEIG, the following assumption was made: the cross-saturation effect is not taken into account; all the machine parameters were considered constant except the magnetizing inductance; iron losses in the machines are not taken into account; the time harmonics effect due to the

action of semiconductor devices in the GIC is not taken into account.

In this study, a mechanical control system for controlling the blade pitch angle in case of the wind speed is more than rated (i.e. 9 m/s) was ignored. For future development, an FLC may be employed by the aid of simulation of the proposed mathematical model for training its FIS in which with any speed more than rated, there is an appropriate pitch angle value for making the value of turbine power within the rated value.

7. Conclusions

1. A mathematical model for the SEIG was implemented by representing the first-order differential equations that describe the currents of both stator and rotor of the machine in addition to the excitation voltages with Matlab/Simulink. Both dynamic and steady-state analysis can be implemented with this model. These analyses provide the required knowledge for the reliable operation of the SEIG.

2. The design and modelling of the wind turbine were done by representing the different equations of the aero model. With the simulation of SEIG-WT, the dynamic of rotor speed change, which influences the stability of both magnitude and frequency of generated voltage, can be noted.

3. The trained (FIS)s had been successfully employed in controlling the parameters of the GIC, i. e. the MI and δ, such that by employing the GIC-FLC in controlling the SEIG-WT, the voltage and frequency were kept with a maximum change of (±1 %) for the voltage and (±0.2 %) for the frequency as a percentage of rated values, for a variety of wind speeds in the range of 7 to 9 m/sec, at a resistive load in the range of 45 to 150 Ω, and inductive load in the range of 10 to 60 mH.

References

1. Chen, J., Wang, F., Stelson, K. A. (2018). A mathematical approach to minimizing the cost of energy for large utility wind turbines. Applied Energy, 228, 1413–1422. doi: https://doi.org/10.1016/j.apenergy.2018.06.150
2. Chatterjee, S., Chatterjee, S. (2018). Review on the techno-commercial aspects of wind energy conversion system. IET Renewable Power Generation, 12 (14), 1581–1608. doi: https://doi.org/10.1049/iet-rpg.2018.5197
3. Kaniuk, G., Vasylets, T., Varfolomiyev, O., Mezerya, A., Antonenko, N. (2019). Development of neuralnetwork and fuzzy models of multimass electromechanical systems. Eastern-European Journal of Enterprise Technologies, 3 (2 (99)), 51–63. doi: https://doi.org/10.15587/1729-4061.2019.169080
4. Murthy, S. S., Pinto, A. J. P. (2005). A generalized dynamic and steady state analysis of self excited induction generator (SEIG) based on MATLAB. 2005 International Conference on Electrical Machines and Systems, 3, 1933–1938. doi: https://doi.org/10.1109/icems.2005.202898
5. Basic, M., Vukadinovic, D. (2016). Online Efficiency Optimization of a Vector Controlled Self-Excited Induction Generator. IEEE Transactions on Energy Conversion, 31 (1), 373–380. doi: https://doi.org/10.1109/tec.2015.2492601
6. Mahajan, S. M., Senthil Kumar, S., Kumaresan, N., Ammasai Gounden, N. G., Rajkumar, E. (2016). Decoupled control strategy for the operation of capacitor-excited induction generator for DC power applications. IET Power Electronics, 9 (13), 2551–2561. doi: https://doi.org/10.1049/iet-pel.2015.0830
7. Scherer, L. G., de Camargo, R. F., Tambara, R. V. (2016). Voltage and frequency regulation of standalone self-excited induction generator for micro-hydro power generation using discrete-time adaptive control. IET Renewable Power Generation, 10 (4), 531–540. doi: https://doi.org/10.1049/iet-rpg.2015.0321
8. Ezzeddine, T. (2020). Reactive power analysis and frequency control of autonomous wind induction generator using particle swarm optimization and fuzzy logic. Energy Exploration & Exploitation, 38 (3), 755–782. doi: https://doi.org/10.1177/0144598719886373
9. Seyoum, D., Grantham, C., Rahman, M. F. (2003). The dynamic characteristics of an isolated self-excited induction generator driven by a wind turbine. IEEE Transactions on Industry Applications, 39 (4), 936–944. doi: https://doi.org/10.1109/tia.2003.813738
10. Jayalakshmi, N. S., Gaonkar, D. N. (2012). Dynamic modeling and analysis of an isolated self excited induction generator driven by a wind turbine. 2012 International Conference on Power, Signals, Controls and Computation. doi: https://doi.org/10.1109/epscicon.2012.6175250
11. Wang, H., Wu, X., You, R., Li, J. (2018). Modeling and analysis of SEIG-STATCOM systems based on the magnitude-phase dynamic method. Journal of Power Electronics, 18 (3), 944–953. doi: https://doi.org/10.6113/JPE.2018.18.3.944
12. Chilipi, R. R., Singh, B., Murthy, S. (2012). A New Voltage and Frequency Controller for Standalone Parallel Operated Self Excited Induction Generators. International Journal of Emerging Electric Power Systems, 13 (1), 1–17. doi: https://doi.org/10.1515/1553-779x.2809
13. Dhanapal, S., Anita, R. (2016). Voltage and Frequency Control of Stand Alone Self-Excited Induction Generator Using Photovoltaic System Based STATCOM. Journal of Circuits, Systems and Computers, 25 (04), 1650031. doi: https://doi.org/10.1142/s0218126616500316
14. Singh, B., Kasal, G. K. (2008). Solid State Voltage and Frequency Controller for a Stand Alone Wind Power Generating System. IEEE Transactions on Power Electronics, 23 (3), 1170–1177. doi: https://doi.org/10.1109/tpel.2008.921190

15. Ishchenko, A., Myrzik, J. M. A., Kling, W. L. (2007). Linearization of Dynamic Model of Squirrel-Cage Induction Generator Wind Turbine. 2007 IEEE Power Engineering Society General Meeting. doi: https://doi.org/10.1109/pes.2007.386079
16. Venkatesa Perumal, B., Chatterjee, J. K. (2006). Analysis of a self excited induction generator with STATCOM/battery energy storage system. 2006 IEEE Power India Conference. doi: https://doi.org/10.1109/poweri.2006.1632596
17. Chatterjee, J. K., Perumal, B. V., Gopu, N. R. (2007). Analysis of Operation of a Self-Excited Induction Generator With Generalized Impedance Controller. IEEE Transactions on Energy Conversion, 22 (2), 307–315. doi: https://doi.org/10.1109/tec.2006.875432
18. Dalei, J., Mohanty, K. B. (2016). An approach to estimate and control SEIG voltage and frequency using CORDIC algorithm. Transactions of the Institute of Measurement and Control, 39 (6), 861–871. doi: https://doi.org/10.1177/0142331215621374
19. Farret, F. A., Palle, B., Simoes, M. G. (2004). State space modeling of parallel self-excited induction generators for wind farm simulation. Conference Record of the 2004 IEEE Industry Applications Conference, 2004. 39th IAS Annual Meeting, 4, 2801–2807. doi: https://doi.org/10.1109/ias.2004.1348870
20. Xia, Y., Ahmed, K. H., Williams, B. W. (2013). Wind Turbine Power Coefficient Analysis of a New Maximum Power Point Tracking Technique. IEEE Transactions on Industrial Electronics, 60 (3), 1122–1132. doi: https://doi.org/10.1109/tie.2012.2206332
21. Goel, P. K., Singh, B., Murthy, S. S., Kishore, N. (2011). Isolated Wind–Hydro Hybrid System Using Cage Generators and Battery Storage. IEEE Transactions on Industrial Electronics, 58 (4), 1141–1153. doi: https://doi.org/10.1109/tie.2009.2037646
22. Singh, B., Murthy, S. S., Gupta, S. (2004). Analysis and Design of STATCOM-Based Voltage Regulator for Self-Excited Induction Generators. IEEE Transactions on Energy Conversion, 19 (4), 783–790. doi: https://doi.org/10.1109/tec.2004.827710
23. Sakkoury, K. S., Emara, S., Ahmed, M. K. (2017). Analysis of wind driven self-excited induction generator supplying isolated DC loads. Journal of Electrical Systems and Information Technology, 4 (1), 257–268. doi: https://doi.org/10.1016/j.jesit.2016.08.003